Int. J. Heat Mass Transfer. Vol. 33, No. 6, pp. 1359–1362, 1990
Printed in Great Britain

0017-9310/90 $3.00+0.00

TECHNICAL NOTES

Effect of a 180° bend on heat transfer in a downstream positioned straight tube

M. M. OHADI
Department of Mechanical Engineering and Engineering Mechanics, Michigan Technological University, Houghton, MI 49931, U.S.A.

and

E. M. SPARROW
Department of Mechanical Engineering, University of Minnesota, Minneapolis, MN 55455, U.S.A.

(*Received* 13 *July* 1989 *and in final form* 19 *September* 1989)

INTRODUCTION

THE PURPOSE of this Technical Note is to convey newly obtained data to make more complete a prior paper [1] by the authors dealing with heat or mass transfer in a straight tube downstream of a bend. Owing to a gap of more than three years between the original investigation and the recent follow-on work, it was not possible to report the newly obtained results in ref. [1]. In ref. [1], the bends used in the experiments had turn angles of 0 (no bend), 30, 60, and 90°, while the present results correspond to a bend with a 180° turn angle.

In addition to the parametric variation of the bend turn angle, two other parameters were varied during the course of the experiments. One of these is the tube Reynolds number, which ranged from about 5000 to about 80 000. The other parameter is the flow condition at the bend inlet. For one inlet condition, the bend is fed by an upstream-positioned hydrodynamic development tube, while in a second inlet condition, the bend is fed from a large upstream plenum chamber through a sharp-edged inlet. These two conditions are respectively denoted as the tube-fed bend inlet and the sharp-edged bend inlet.

The bend—its turn angle and its inlet configuration—governed the nature of the fluid flow presented to a straight tube situated downstream of the bend. The tube was designed and instrumented to provide local mass transfer coefficients and local Sherwood numbers as a function of axial position along its length. The mass transfer measurements were performed using the naphthalene sublimation technique, with air as the working fluid. As is well known, Nusselt numbers for heat transfer can be deduced from mass transfer Sherwood numbers by making use of the analogy between heat and mass transfer. The Schmidt number, which is the mass transfer analogue of the Prandtl number, is 2.5 for the naphthalene–air system. In neither the present experiments nor in ref. [1] did mass transfer occur upstream of the straight tube (analogous to adiabatic conditions upstream of the tube for the corresponding heat transfer problem). The mass transfer boundary condition at the tube wall corresponds to a uniform wall temperature in the heat transfer analogue.

The details of the experimental apparatus, operating procedure, and data reduction are described in detail in ref. [1] and need not be repeated here. It should be noted, however, that the present version of the apparatus is somewhat enhanced compared with that employed in ref. [1]. Subsequent to the completion of ref. [1], the mass transfer test section was transported from the University of Minnesota to the Michigan Technological University, where three additional mass transfer elements were installed to extend its length from 20.4 to 25.2 diameters.

RESULTS AND DISCUSSION

The local mass transfer results will be reported here in dimensionless form in terms of the local Sherwood number, which is defined as

$$Sh = KD/\mathscr{D} \tag{1}$$

where K is the local mass transfer coefficient, D the tube inside diameter, and $\mathscr{D}$ the mass diffusion coefficient. The Sherwood number distributions will be plotted as a function of the dimensionless axial coordinate X/D, where the origin of X coincides with the upstream end of the mass transfer tube. The tube Reynolds number, which serves to parameterize the data, has its standard definition

$$Re = 4\dot{w}/\mu\pi D \tag{2}$$

with $\dot{w}$ denoting the mass flow rate of the air and μ the air viscosity.

The axial distributions of the local Sherwood number corresponding to the 180° bend turn angle constitute the new results of this investigation. These results are presented in Figs. 1 and 2 as Sh vs X/D. The first of these figures covers the lower Reynolds numbers in the investigated range, while the second figure covers the upper Reynolds numbers in the range. In addition to the Reynolds number parameterization of the data in each figure, the flow condition at the bend inlet also serves as a parameter, respectively characterized by open and black symbols for the tube-fed and sharp-edged inlets.

An overall inspection of Figs. 1 and 2 reveals a significant difference in the nature of the axial distributions of the Sherwood number in the two figures. In Fig. 1, which pertains to the lower Reynolds numbers ($Re \sim$ 5000–15 000), the Sherwood number decreases at first and attains a minimum, whereafter it increases and subsequently approaches an axially unchanging, fully developed value. Thus, each distribution in Fig. 1 undershoots the fully developed value before recovering. On the other hand, for the Reynolds numbers of Fig. 2, which range from about 24 000 to about 77 000, the Sherwood number decreases monotonically with increasing downstream distance along the tube and approaches the fully developed value from above (i.e. no undershoot).

NOMENCLATURE

- D internal diameter of tube
- $\mathcal{D}$ mass diffusion coefficient
- K local mass transfer coefficient
- Re Reynolds number, $4\dot{w}/\mu\pi D$
- Sh Sherwood number, $KD/\mathcal{D}$
- $\dot{w}$ mass flow rate of air
- X axial coordinate in mass transfer tube.

Greek symbol
- μ viscosity.

The aforementioned unconventional behavior of the Sherwood number distributions at lower Reynolds numbers (i.e. the undershoot) had already been observed in ref. [1] at Reynolds numbers of $\sim$5400 and 9100 in the presence of the 90° turn angle bend and also at Re $\sim$5400 for the 60° turn angle bend with a sharp-edged inlet. However, the Sherwood number distributions of ref. [1] for Re $\sim$15000 did not exhibit undershoot. In contrast, the present Re $\sim$15000 Sherwood number distributions, which correspond to a 180° turn angle bend, display the undershoot phenomenon. Thus, the attainment of Sherwood number undershoot at higher Reynolds numbers is facilitated by larger bend turn angles.

As discussed in ref. [1], the cause of the undershoot is the laminarization of the flow and the subsequent transition to turbulence—the laminarization being responsible for the relatively low Sherwood numbers and the transition for the subsequent recovery of the Sherwood numbers. Earlier fluid flow studies (cited in ref. [1]) had demonstrated that a turbulent flow entering a curved tubular element such as a coiled tube or a bend may emerge from the curved element in a laminarized state. The extent of the laminarization depends on the length of run of the flow in the curved element and also on the magnitude of the Reynolds number. The longer the length of run, the greater is the expected degree of laminarization. Also, the lower the Reynolds number of the entering turbulent flow, the more susceptible it should be to being laminarized.

The fact that laminarization is observed here for Re $\sim$15000 and was not encountered for that Reynolds number in ref. [1] adds quantitative support to the aforementioned qualitative characteristic that the degree of laminarization is enhanced by longer lengths of curved flow, i.e. larger bend turn angles. The absence of data for Reynolds numbers between 15000 and 24000 makes it difficult to pinpoint at which Re value the laminarization effect disappears, but it is definitely in that range.

Figure 1 clearly indicates support for the assertion that the degree of laminarization increases as the Reynolds number of the initially turbulent flow decreases. In particular, at Re $\sim$5300, the process of laminarization and subsequent retransition to turbulence requires a length of almost 20 diameters for its completion, while the corresponding lengths for the Reynolds numbers of about 10000 and 15000 are approximately 13 and 10 diameters, respectively. The respective Sherwood number minima for the three Reynolds numbers occur at 7, 5, and 3.5 diameters. At these locations, the corresponding undershoots, relative to their respective fully developed Sherwood numbers, are about 34, 24, and 12%. The quantification of the laminarization effect caused by a 180° bend is a major result of this investigation.

Attention may now be directed to a comparison of the Sherwood number distributions of Figs. 1 and 2 for the tube-fed and sharp-edged bend inlets. An overview of the figures indicates that all of the trendwise characteristics are common to the two sets of distributions and, in the main, even the magnitudes of the Sherwood numbers are in close agreement. These observations make physical sense since the relatively long 180° bend serves to shield the mass transfer tube from the specifics of the flow condition at the bend inlet. In particular, the present Sherwood number results, which correspond to a 180° bend, should be less influenced by the bend inlet conditions than are the results of ref. [1], which were for bends having turn angles of 90° and less.

Aside from the small, apparently aberrant deviations for Re $\sim$9800–9900, the Sherwood numbers corresponding to the two bend inlet conditions are virtually identical for $X/D > 5$. For $X/D < 5$, the two data sets continue to track each other very well, aside from deviations at a restricted

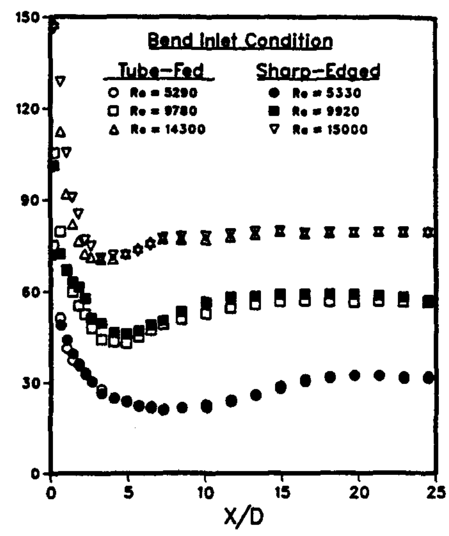

FIG. 1. Axial distributions of the local Sherwood number in a tube situated downstream of a 180° bend, $Re \sim 5000$–15000.

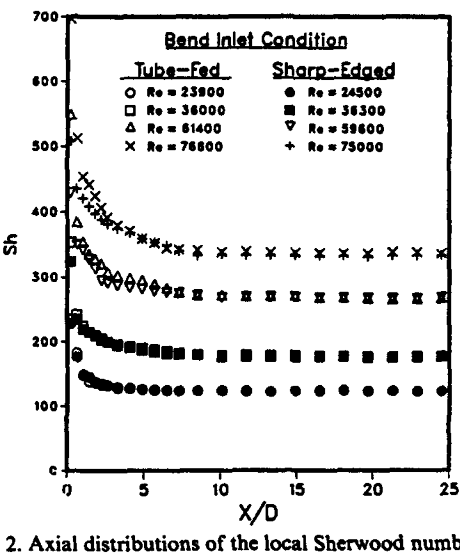

FIG. 2. Axial distributions of the local Sherwood number in a tube situated downstream of a 180° bend, $Re \sim 24000$–77000.

number of points. Significant deviations occur at the first two measurement stations for the highest Reynolds number and at the first measurement station for the next-to-highest Reynolds number. Note that these stations are situated in the range $X/D < 1$. It is believed that these deviations are true reflections of the different bend inlet conditions. Other deviations, such as those at small X/D for $Re \sim 15\,000$, are believed to be due to data scatter.

The foregoing presentation and discussion was focused on the Sherwood number results in the presence of a 180° bend. Now, attention will be turned to comparing these results with those corresponding to other bend turn angles. Such comparisons are made for three representative Reynolds numbers in Figs. 3 and 4. Figure 3 is for the case of the tube-fed bend inlet, while Fig. 4 is for the sharp-edged bend inlet. Each figure is subdivided into (a), (b), and (c) parts, which respectively convey results for nominal Reynolds numbers of 5500, 24 000, and 60 000. In each figure, axial distributions of the Sherwood number are plotted for five bend turn angles: 0 (no bend), 30, 60, 90, and 180°. The data for the first four of these were presented in ref. [1], while the 180° data comprise the present contribution.

The discussion will begin with Fig. 3. At the lowest investigated Reynolds number of about 5500 (Fig. 3(a)), the dominant feature is the laminarization-related undershoot of the Sherwood number and its subsequent recovery as the flow experiences retransition to turbulence. These events occur in the presence of both the 90 and 180° bend turn angles, but not for the others. The laminarization effect is more pronounced with the 180° bend in place than with the 90° bend in place (i.e. a deeper minimum), but the data for the two cases merge during the recovery and attain the same fully developed Sherwood number. This fully developed value is somewhat higher than those attained with the smaller turn angle bends in place, suggesting that a different turbulence structure may result from the laminarization and subsequent retransition. Note that the 180° data extend to larger X/D than do the other data because a longer mass transfer tube was used in the present experiments.

At the higher Reynolds numbers (24 000 and 60 000) of Figs. 3(b) and (c), the fully developed Sh values corresponding to the 180° bend continue to fall higher than the others (including the 90° data). Although there is no evident laminarization and retransition at these Reynolds numbers, it appears that a relatively long length of run through a bend can influence the turbulence in a tube situated downstream of the bend. This influence may be masked in the entrance region of the tube by the different redevelopment patterns experienced by differently turned flows. Evidence of these different redevelopment patterns is provided in Figs. 3(b) and (c) by the considerable spread among the entrance region data corresponding to the different turn angles.

The discussion will now be redirected from Fig. 3 to Fig. 4. In considering Fig. 4, it should be noted that the no-bend case (0° turn angle) displays a special behavior at small X/D because the sharp-edged inlet is situated directly at the upstream end of the mass transfer tube. The associated separation of the flow at the tube inlet and the subsequent reattachment gives rise to a Sherwood number distribution which increases at first, attains a maximum, and then decreases monotonically to a fully developed value. With a bend in place, the sharp-edged-inlet-related separation occurs upstream of the mass transfer tube (i.e. in the bend), so that the Sherwood number distributions are monotonically decreasing in the range of small X/D.

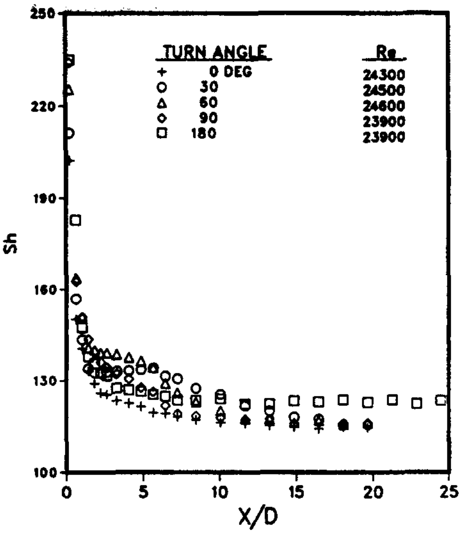

FIG. 3(b). Effect of bend turn angle on the Sherwood number distribution in a tube situated downstream of a bend with a tube-fed inlet, $Re \sim 24\,000$.

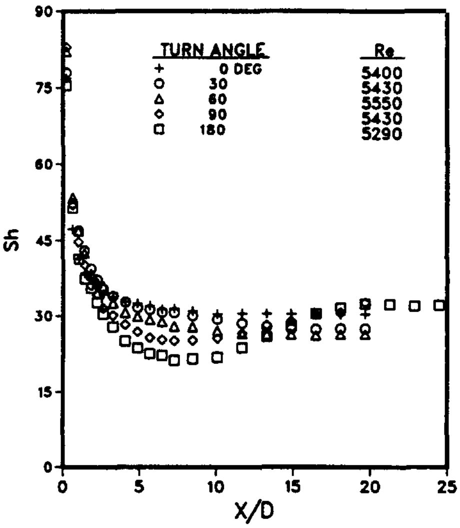

FIG. 3(a). Effect of bend turn angle on the Sherwood number distribution in a tube situated downstream of a bend with a tube-fed inlet, $Re \sim 5500$.

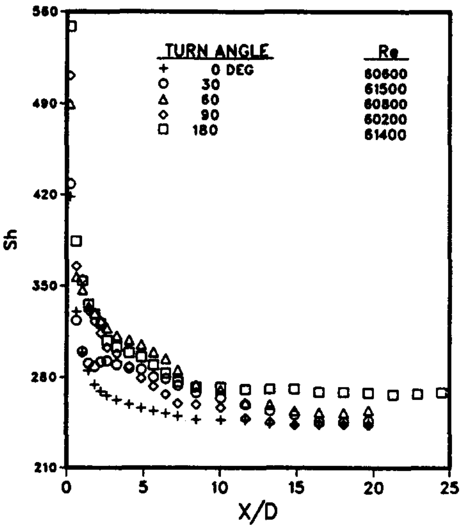

FIG. 3(c). Effect of bend turn angle on the Sherwood number distribution in a tube situated downstream of a bend with a tube-fed inlet, $Re \sim 60\,000$.

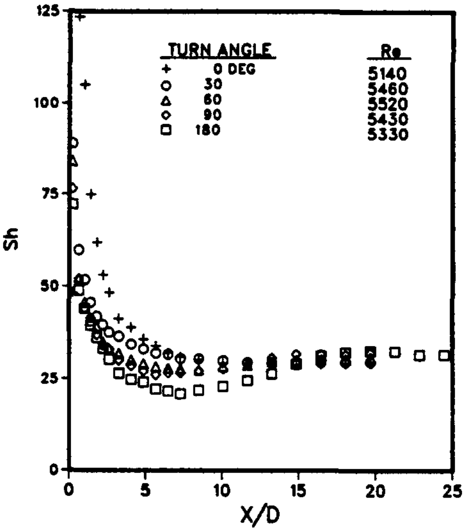

FIG. 4(a). Effect of bend turn angle on the Sherwood number distribution in a tube situated downstream of a bend with a sharp-edged inlet, $Re \sim 5500$.

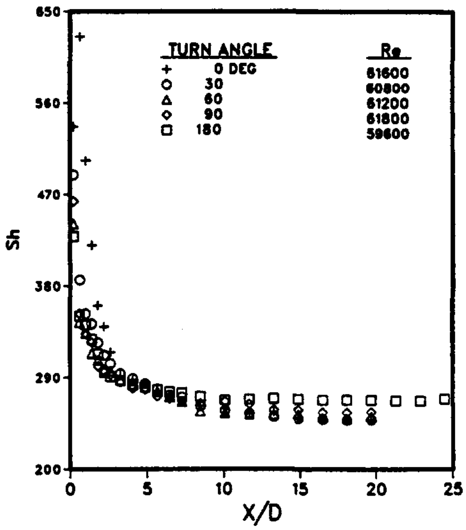

FIG. 4(c). Effect of bend turn angle on the Sherwood number distribution in a tube situated downstream of a bend with a sharp-edged inlet, $Re \sim 60\,000$.

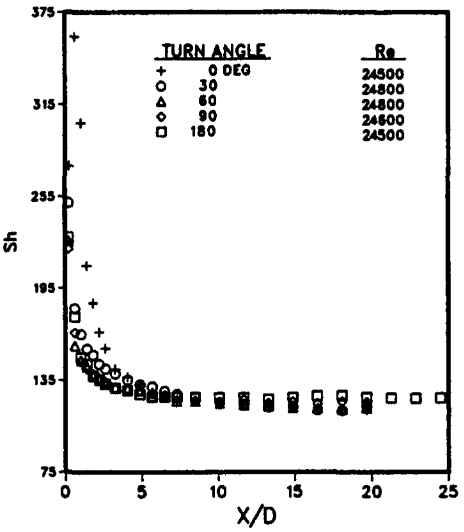

FIG. 4(b). Effect of bend turn angle on the Sherwood number distribution in a tube situated downstream of a bend with a sharp-edged inlet, $Re \sim 24\,000$.

The laminarization–retransition sequence for the 90 and 180° cases that was already discussed in connection with Fig. 3(a) is repeated in Fig. 4(a). In addition, the 60° case in Fig. 4(a) displays the same sequence, albeit to a muted extent. Also noteworthy is that the fully developed *Sh* values for the various turn angle cases in Fig. 4(a) are in closer mutual agreement than are those of Fig. 3(a).

If the unique behavior of the no-bend case is excluded from consideration, it may be observed that the Sherwood number distributions of Figs. 4(b) and (c) fall in a tighter band than do their counterparts in Figs. 3(b) and (c), even taking into account the differences in the ordinate scales. Thus, the entrance region Sherwood numbers appear to be less sensitive to the magnitude of the turn angle when the bend has a sharp-edged inlet. As was also true in Figs. 3(b) and (c), the fully developed Sherwood numbers for the 180° bend fall above the others in Figs. 4(b) and (c). However, the deviations are now somewhat smaller, in accord with the aforementioned reduced sensitivity to the turn angle.

REFERENCE

1. M. M. Ohadi and E. M. Sparrow, Heat transfer in a straight tube situated downstream of a bend, *Int. J. Heat Mass Transfer* 32, 201–212 (1989).